

Finite element analysis of steel fiber-reinforced concrete (SFRC): validation of experimental tensile capacity of dog-bone specimens

Md. Mashfiqul Islam · Md. Arman Chowdhury ·
Md. Abu Sayeed · Elsha Al Hossain ·
Sheikh Saleh Ahmed · Ashfia Siddique

Received: 29 November 2013 / Accepted: 17 June 2014 / Published online: 1 August 2014
© The Author(s) 2014. This article is published with open access at Springerlink.com

Abstract Finite element analyses are conducted to model the tensile capacity of steel fiber-reinforced concrete (SFRC). For this purpose dog-bone specimens are casted and tested under direct and uniaxial tension. Two types of aggregates (brick and stone) are used to cast the SFRC and plain concrete. The fiber volume ratio is maintained 1.5 %. Total 8 numbers of dog-bone specimens are made and tested in a 1000-kN capacity digital universal testing machine (UTM). The strain data are gathered employing digital image correlation technique from high-definition images and high-speed video clips. Then, the strain data are synthesized with the load data obtained from the load cell of the UTM. The tensile capacity enhancement is found 182–253 % compared to control specimen to brick SFRC and in case of stone SFRC the enhancement is 157–268 %. Fibers are found to enhance the tensile capacity as well as ductile properties of concrete that ensures to prevent sudden brittle failure. The dog-bone specimens are modeled in the ANSYS 10.0 finite element platform and analyzed to model the tensile capacity of brick and stone SFRC. The SOLID65 element is used to model the SFRC as well as plain concretes by optimizing the Poisson's ratio, modulus of elasticity, tensile strength and stress–strain relationships and also failure pattern as well as failure locations. This research provides information of the tensile capacity enhancement of SFRC made of both brick and stone which will be helpful for the construction industry of Bangladesh to introduce this engineering material in earthquake design. Last of all, the finite element outputs are found to hold

good agreement with the experimental tensile capacity which validates the FE modeling.

Keywords Finite element analyses (FEA) · Steel fiber-reinforced concrete (SFRC) · Dog-bone specimens · Tensile capacity of concrete

Introduction

Concrete shows a low tensile strength in comparison to the compressive strength, which grows only less proportionally with increasing compressive strength; at the same time, the brittleness increases. Therefore, fibers are added to improve ductility and to increase the tensile strength. For many applications, however, conventional reinforcement in the tensile zone is still necessary. Fibers are increasingly being used in concrete structures to compensate for concrete's weak and brittle tensile behavior relative to its compression response. One of the most beneficial aspects of the use of fibers in concrete structures is that non-brittle behavior after concrete cracking can be achieved with fibers. The tensile stress sustainable in concrete rapidly decreases immediately after cracking. In fiber-reinforced concrete (FRC), on the other hand, fibers crossing the crack interfaces significantly contribute to the load-carrying mechanism so that considerable tensile stress, being the sum of the tensile resistance provided by fibers and tension softening of the concrete matrix, respectively, can be achieved even with large crack widths (Lee et al. 2011). Therefore, the enhanced tensile stress behavior attainable with fibers should be realistically evaluated to accurately predict the post-cracking response of FRC. The bond resistance of reinforcing bars embedded in concrete depends primarily on frictional resistance and mechanical

M. M. Islam (✉) · M. A. Chowdhury · M. A. Sayeed ·
E. A. Hossain · S. S. Ahmed · A. Siddique
Department of Civil Engineering, Ahsanullah University of
Science and Technology (AUST), Dhaka 1208, Bangladesh
e-mail: mashfiq7777@gmail.com; mashfiq7777@yahoo.com



interlock. The chemical adhesion bond, if any, fails at very small slips. Frictional bond provides initial resistance against loading and further loading mobilizes the mechanical interlock between the concrete and bar ribs. Mechanical interlock leads to inclined bearing forces, which in turn leads to transverse tensile stresses and internal inclined splitting (bond) cracks along reinforcing bars (Chao et al. 2009). To this end, this research modeled direct tensile strength of plain concrete and steel fiber-reinforced concrete (SFRC) in Finite Element platform and are evaluated based on experimental investigation.

The ANSYS 10.0 Finite Element Analysis (FEA) software package is used to analyze the direct tension specimens and introduces a good concrete model for Steel Fiber-Reinforced Concrete (SFRC) as well as plain concrete made of brick and stone aggregate. Two different Poisson's ratios for brick and stone concrete are selected by comparing FE output with the stress–strain behavior in tension. A reasonable modeling of concrete using suitable element type,

adequate mesh size, appropriate boundary conditions, realistic loading environment and proper time stepping can help to estimate the governing parameters of concrete. Using these governing parameters (i.e. Poisson's ratio, tensile strength, and the stress–strain relationship), the dog-bone tensile specimens are modeled, analyzed and compared the results gathered from experimental outcomes. After evaluation of this parameter by extensive analysis, Finite Element (FE) models showed a good correlation with the experimental results and also showed similar failure patterns. This investigation is intended to validate the FE models with the experimental results by identifying and using the pertinent parameters of the concrete model as well as to provide a successful FE SFRC model for analyzing future problems on SFRC and in context of Bangladesh. The current research aims to investigate the capacity enhancement and stress field of the SFRC from experimental and numerical viewpoint to introduce this new engineering material in the construction industries of Bangladesh.

Fig. 1 Experimental test setup: **a** UTM and customized tension frame, **b** failed plain brick concrete dog-bone specimen

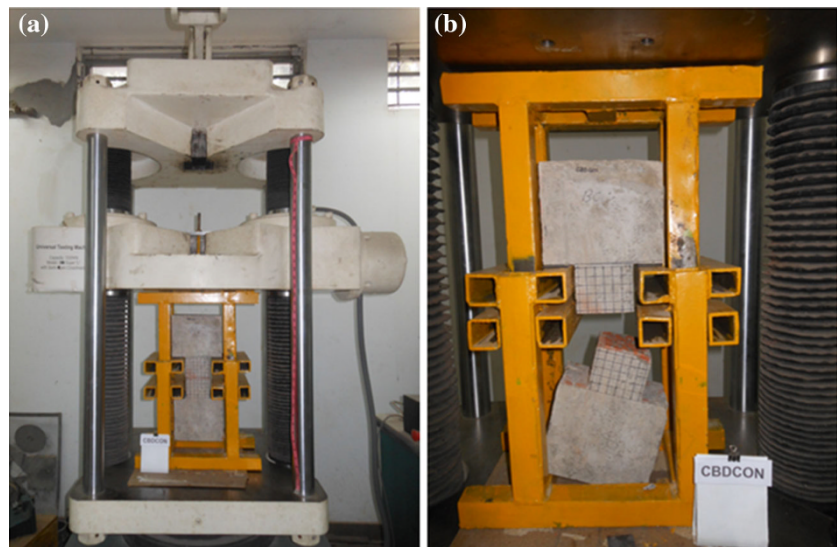
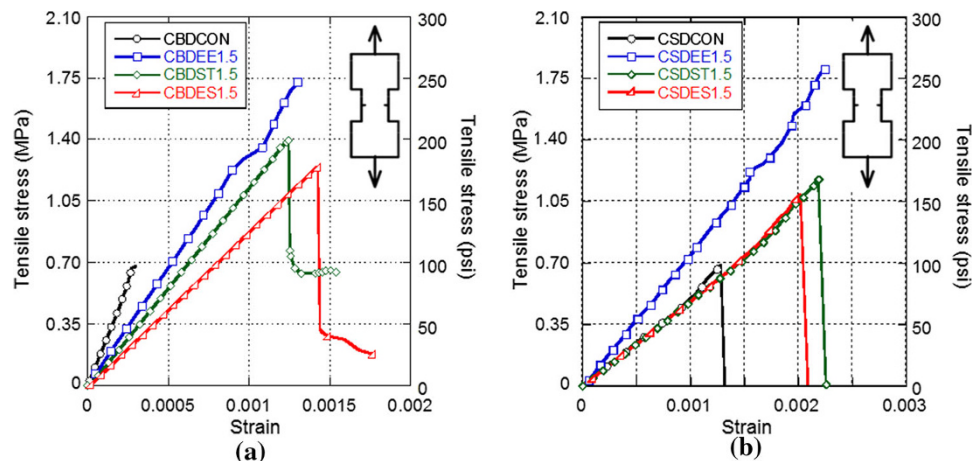


Fig. 2 Tensile stress–strain behavior of plain concrete and SFRC: **a** brick concrete, **b** stone concrete



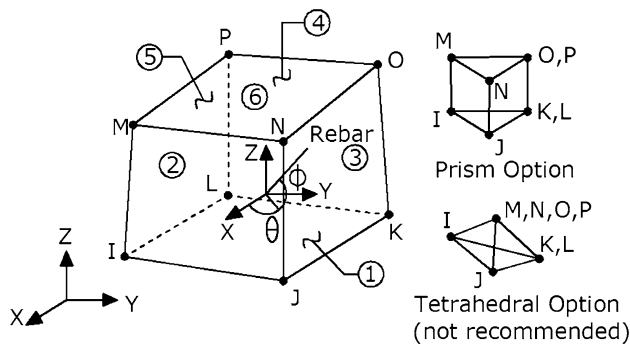


Fig. 3 Geometry of SOLID65 in ANSYS 10.0 platform

Experimental program

In this research, dog-bone specimens are introduced to determine direct tensile strength of plain concrete and SFRC. Two kinds of SFRC and plain concretes, brick (represented as CB in specimen designation) and stone (CS), are tested experimentally and also modeled in FE platform. The fiber volume is taken as 1.5 % (represented as 1.5 in specimen designation) to cast the tensile

specimens. Enlarged end fibers (EE) showed good performance in tensile capacity enhancement compared to straight fibers (ST) and mixed fibers (ES) of small and enlarged ends. The fibers are customized to make enlarged ends for better anchorage. The dog-bone specimens are notched at the middle of the web in four sides which acted as stress concentrator as well as to control the failure location. All the specimens are tested in a 1000k-N capacity digital universal testing machine (UTM) as shown in Fig. 1. The specimens are tested as displacement control procedure at a displacement rate of 0.5 mm/min. Strain data are measured by applying digital image correlation technique (DICT) using high-definition (HD) images and high-speed video clips, and these data are synthesized with the load data from the load cell of UTM which is also followed in the work of Islam (2011), Islam et al. (2011), Uddin et al. (2013) and Dola et al. (2013). The tensile capacity enhancement is found to be 253, 204 and 182 % compared to control specimen for brick SFRC made of end enlarged fibers, straight fiber and 50–50 mixed fibers, respectively. These values in case of stone SFRC are 268, 175 and 157 % respectively. Figure 2 shows the tensile stress–strain behavior of plain concrete and SFRC made of

Fig. 4 Uniaxial compressive stress–strain curve: **a** brick concrete, **b** stone concrete and splitting tensile stress–strain curves, **c** brick concrete, **d** stone concrete

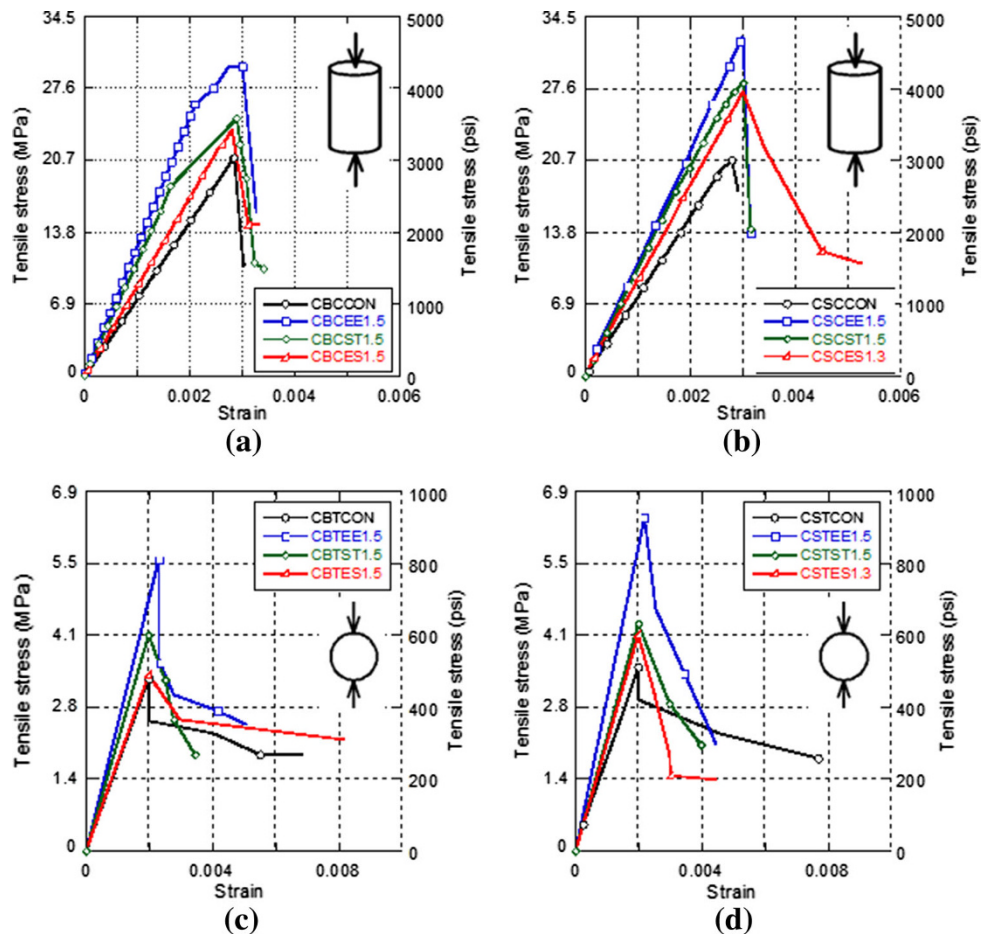
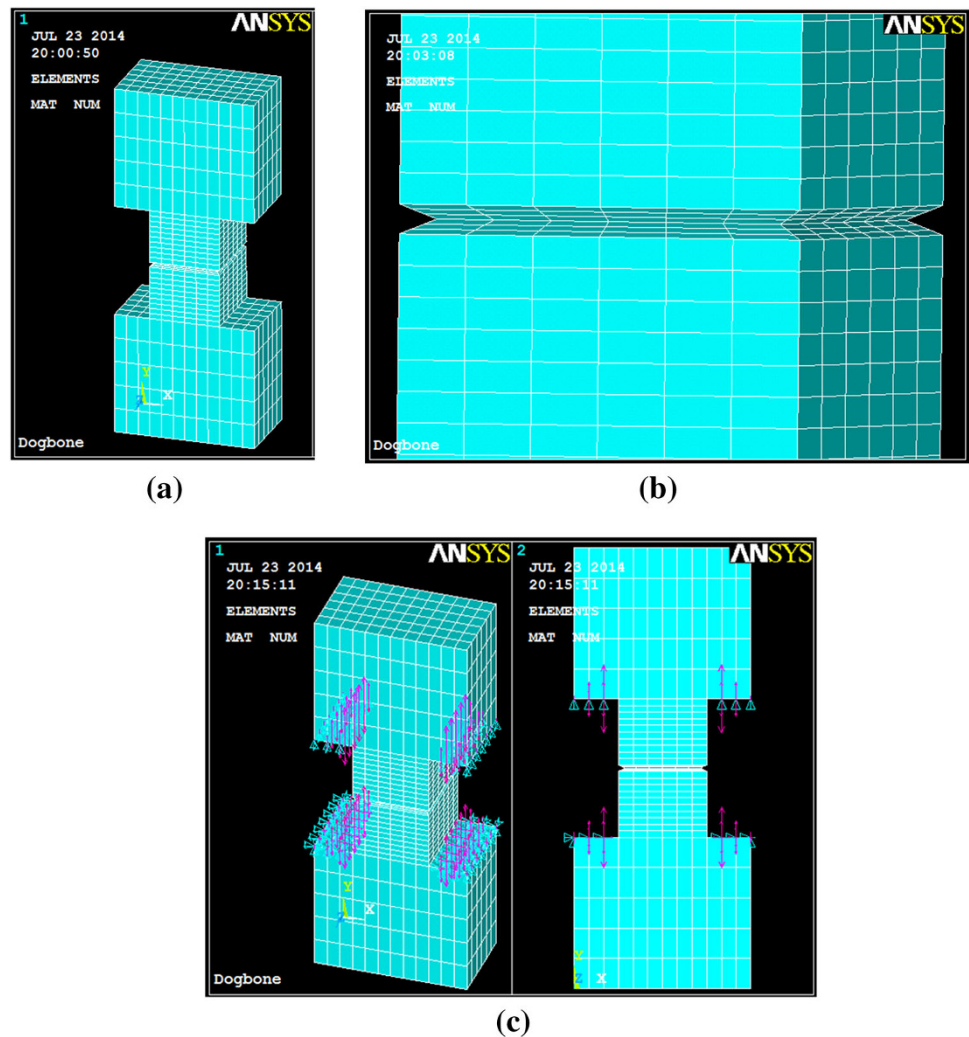


Fig. 5 FE model of dog-bone specimens: **a** full model, **b** close look of notch, **c** boundary conditions



brick and stone concrete. Dog-bone specimens reinforced with enlarged end fibers are then modeled in the FE platform of ANSYS 10.0 and also validated with the experimental results and failure patterns.

Finite element modeling and analysis

All the plain concrete and SFRC dog-bone specimens are modeled on the FE platform of ANSYS 10.0 using an eight-node solid element SOLID65. The element is defined by eight nodes having three degrees of freedom at each node: translations in the nodal x , y , and z directions. The element is capable of plastic deformation, cracking in three orthogonal directions, and crushing. In concrete applications, for example, the solid capability of the element is used to model the concrete while the rebar capability is available for modeling reinforcement behavior. Other cases for which the element is also applicable would be reinforced composites (ANSYS 2005), such as, fiberglass as

well as fiber-reinforced concrete (FRC). The geometry and node locations for SOLID65 element are shown in Fig. 3.

The tensile strength of concrete is typically 8–15 % of the compressive strength (Shah et al. 1995). Figure 4a and b shows the compressive behavior of plain brick concrete, brick SFRC, plain stone concrete and stone SFRC. Again Fig. 4c and d shows the tensile behavior of plain brick concrete, brick SFRC, plain stone concrete and stone SFRC. In tension, the stress–strain curve (Fig. 4c, d) for concrete is approximately linearly elastic up to the maximum tensile strength. After this point, the concrete cracks and strength decrease gradually to zero (Willam and Warnke 1975).

To model concrete and SFRC in ANSYS platform following properties are to be provided, i.e. (i) elastic modulus, (ii) compressive stress–strain relationship, (iii) ultimate uniaxial tensile strength and (iv) Poisson's ratio. All the values are provided from experimental outputs. Poisson's ratio for concrete and SFRC is estimated to be 0.25 and 0.35 for stone and brick concretes respectively by extensive



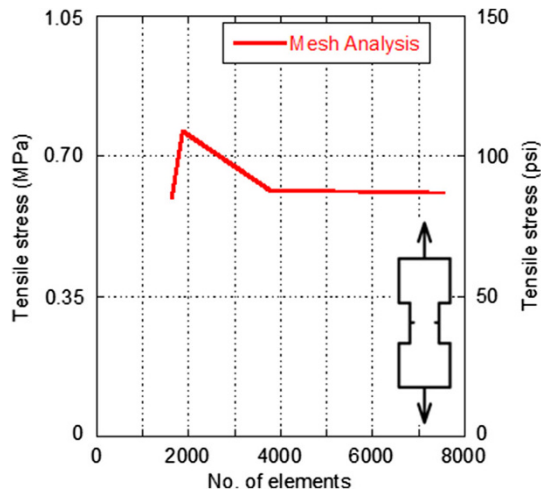


Fig. 6 Stress versus number of elements curve for dog-bone direct tensile specimen

numerical trials and matching experimental data. William and Warnke (William and Warnke 1975) failure criterion is applied to model the concrete as well as SFRC. Four

important parameters, i.e. (i) shear transfer coefficients for an open crack, (ii) shear transfer coefficients for a closed crack, (iii) uniaxial tensile cracking stress and (iv) uniaxial crushing stress are also considered to model the concretes and SFRC. Typical shear transfer coefficients range from 0.0 to 1.0, with 0.0 representing a smooth crack (complete loss of shear transfer) and 1.0 representing a rough crack (no loss of shear transfer). The shear transfer coefficients for open and closed cracks are determined from the work of Kachlakev et al. (2001) as a basis. In the FE models, the values of Poisson's ratio for brick concrete, brick SFRC, stone concrete and stone SFRC applied are 0.4, 0.2, 0.3 and 0.2, respectively; density applied is 0.07, 0.075, 0.07 and 0.075, respectively; shear transfer coefficients for an open crack (β_t) applied are 0.3, 0.3, 0.4 and 0.4, respectively; shear transfer coefficients for a closed crack (β_c) applied are 1.0, 1.0, 0.5 and 1.0, respectively; uniaxial tensile strength applied is 500psi (3.5 MPa), 800psi (5.51 MPa), 500psi (3.5 MPa) and 920psi (6.34 MPa), respectively; and the displacement applied as maintained during experimental testing. The dimension of the web of dog-bone direct

Fig. 7 Validation of FE dog-bone specimens with experimental results: **a** brick plain concrete and **b** brick SFRC with enlarged end fibers

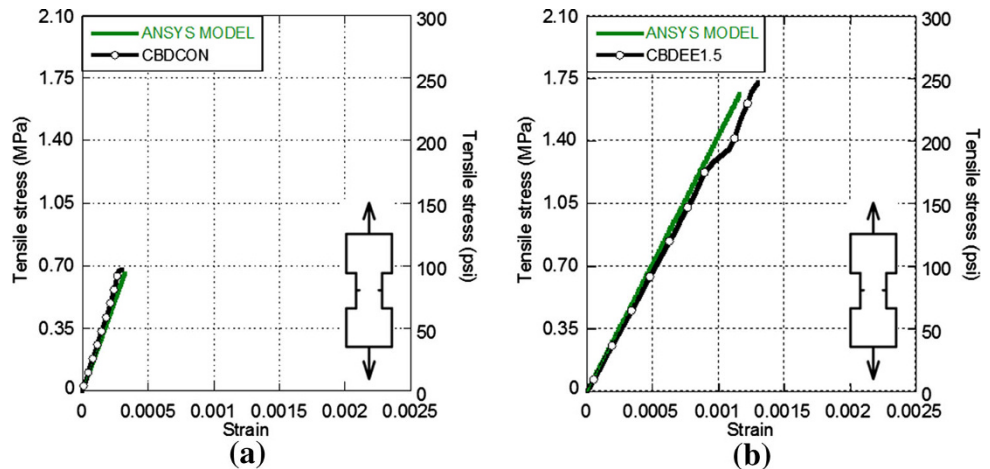
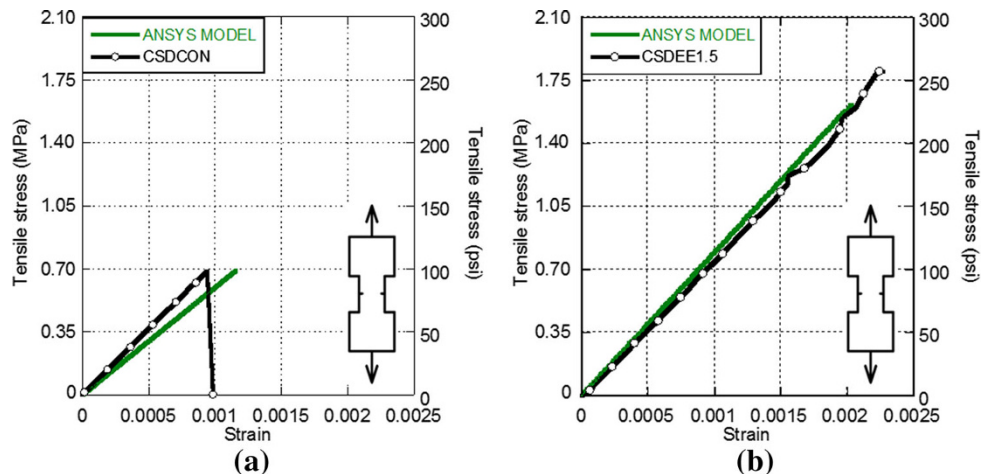


Fig. 8 Validation of FE dog-bone specimens with experimental results: **a** stone plain concrete and **b** stone SFRC with enlarged end fibers



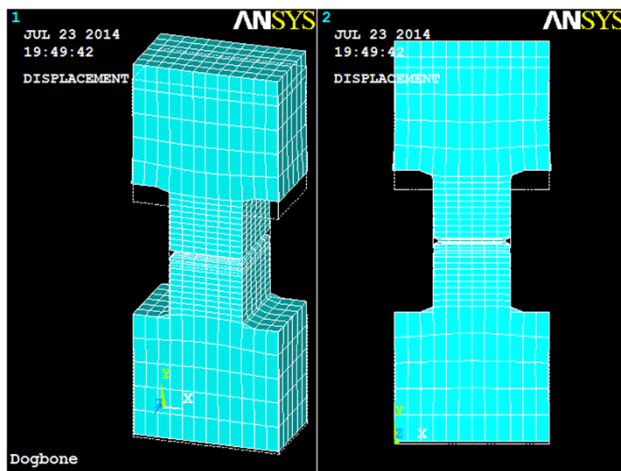


Fig. 9 Deformed shapes

Fig. 10 Stress contours at ultimate collapse situation:
a Y direction stress,
b X direction stress and
c Z direction stress

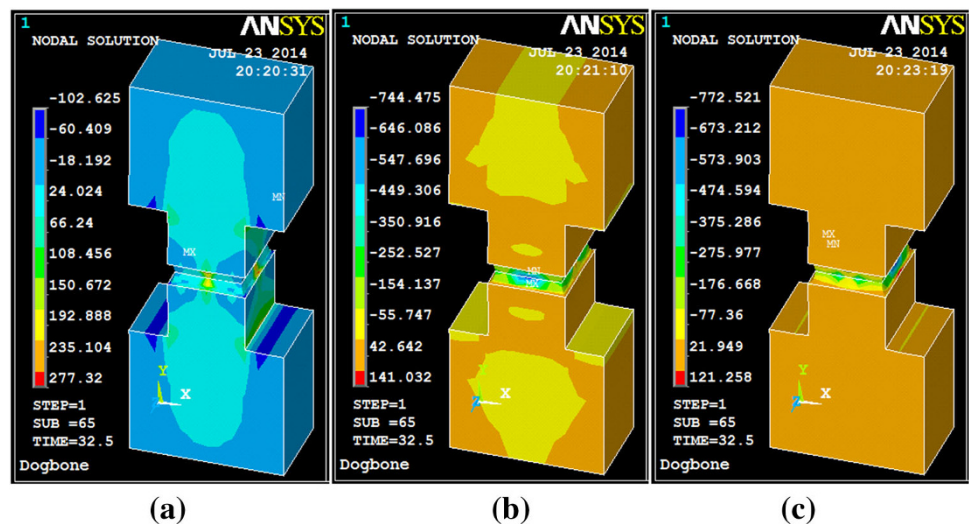
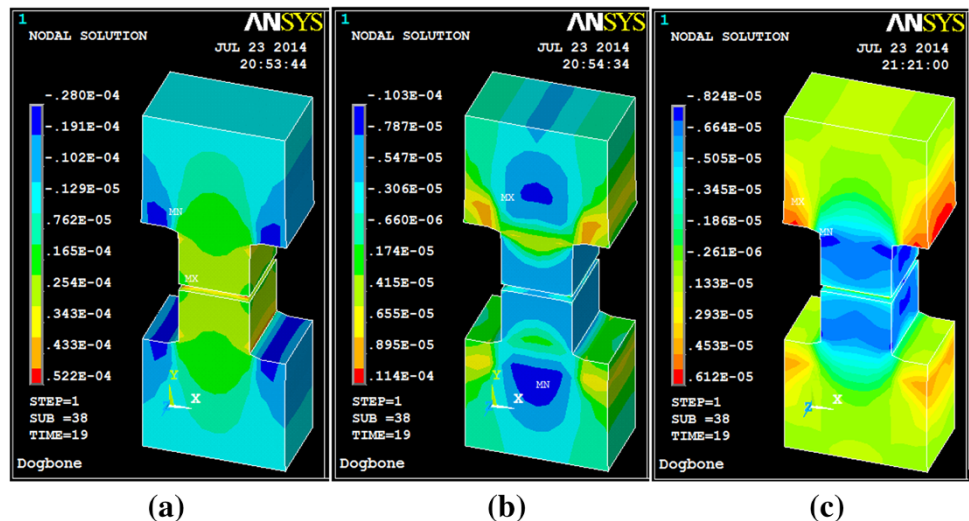


Fig. 11 Strain contours at ultimate collapse situation:
a Y direction strain,
b X direction strain and
c Z direction strain



tension specimens (I shaped with thick flange) are $4 \times 4 \times 5.5$ in ($100 \times 100 \times 140$ mm) attached monolithically with a part of higher stiffness (flange) of size $7 \times 6 \times 4$ in ($178 \times 150 \times 100$ mm) for the gripping the specimens to apply uniaxial tensile force. Loading is applied as displacement boundary condition as experiments are done as displacement control testing. The displacement boundary condition is applied in 500 steps followed by two sub-steps for each step. Figure 5 shows the diagrams of FE models and boundary conditions. The displacement boundary condition is applied at Y direction at the top flange and X, Y, Z direction is restrained at bottom flange.

Adequate mesh size plays an important role in FE analysis. To get the accurate result number of elements versus stress graph is plotted and found interesting relationship between them. Element stress changes with the



increase in number of elements of a specimen, but at a certain ratio stress increasing curve becomes horizontal. It means after a certain number of elements stress will not vary significantly. Figure 6 shows that at a low number of elements stress is changing abruptly whereas at a higher number of elements reaction became stable, but so much higher number of elements will increase the complexity and also the analysis time of the specimen. A reasonable number of elements are selected with maximum accuracy and minimum analysis time. The number of elements taken is 4500 for the FE analyses for dog-bone specimens of both the plain concrete and SFRC.

Validation of finite element models

Validation of tensile capacity

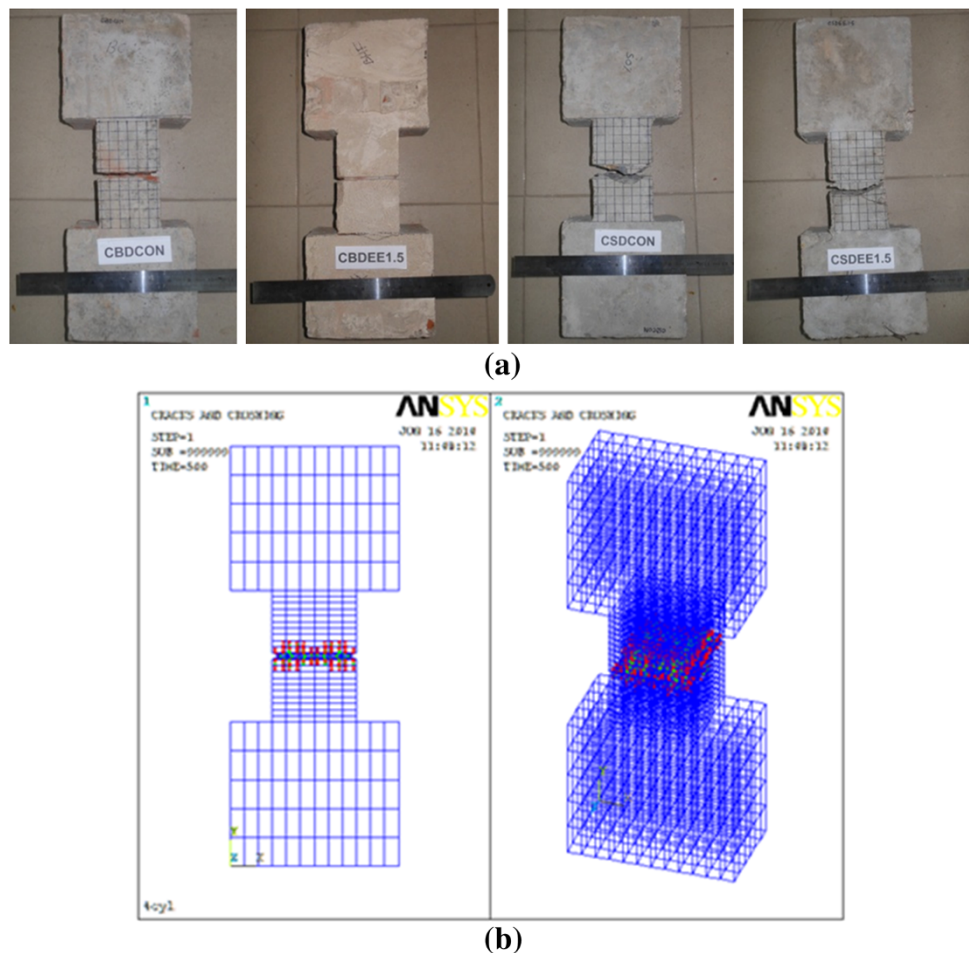
Figures 7 and 8 show the validations of tensile stress results gathered from the experimental measurements with the FE analysis by ANSYS 10.0. It satisfactorily demonstrates the accuracy of the FE model of plain concrete as

well as SFRC made of brick and stone concrete, respectively. The FE results in most of the cases are found to be more or less conservative with respect to the experimental outcomes, which also ensures higher factor of safety as well as reliability of the models. In all the cases the increase of tensile capacity is found which is also seen in the experimental results. The accuracy of the prediction and adjustment of the governing parameters helped to validate the models. The deformed shape is shown in Fig. 9.

Validation of failure pattern

Most of the cracks are formed due to tension and at the notch location. Some SFRC specimens showed crack at the joint of web and flange of the dog-bone specimen (clear from the stress and strain contours of Figs. 10, 11, respectively). The crack is found to be a plane fracture surface in experimental investigation which is also found in ANSYS outputs (Fig. 12). Plain concrete specimens completely separated in two pieces at the notch but SFRC specimens did not. Figure 11 shows the similarities of

Fig. 12 Failure patterns: **a** experimental dog-bone specimens, **b** crack propagation of FE model



failure pattern between the experimental specimen and the FE model using ANSYS. This indicates that the FE modeling of SFRC beam specimens using the pertinent parameters gathered from experimental testing are validated and there remains a good agreement as well as it can be used in future SFRC modeling for tensile loading.

Conclusion

The following conclusions can be drawn from this investigation:

- The tensile capacity enhancement is found to be 253, 204 and 182 % compared to control specimen for brick SFRC made of end enlarged fibers, straight fiber and 50–50 mixed fibers, respectively. These values in case of stone SFRC are 268, 175 and 157 %, respectively.
- The performance of enlarged end fibers showed better capacity enhancements.
- The FE models showed good agreements with the experimental outcomes, which represents the validation of the models.
- The failure patterns found from FE analysis is similar to the experimental results, which also indicates reliable modeling of plain concrete as well as SFRC.
- These FE modeling will definitely provide invaluable information about this engineering material to the construction industry of Bangladesh for future applications.

Open Access This article is distributed under the terms of the Creative Commons Attribution License which permits any use, distribution, and reproduction in any medium, provided the original author(s) and the source are credited.

References

- ANSYS (2005) ANSYS Structural Analysis Guide, Version 10.0, ANSYS, Inc., Canonsburg, Pennsylvania
- Chao S, Naaman AE, Parra-Montesinos GJ (2009) Bond behavior of reinforcing bars in tensile strain-hardening fiber-reinforced cement composites, *ACI Struct J* 106(6):897–906
- Dola JF, Islam MR, Khatun MS, Hussan M (2013) Investigation of the shear capacity of beams made of steel fiber reinforced concrete (SFRC), B.Sc. Engineering Thesis, Department of Civil Engineering, Ahsanullah University of Science and Technology, Dhaka, April
- Islam MM (2011) Interaction diagrams of square concrete columns confined with fiber reinforced polymer wraps, M.Sc. Engineering Thesis, Department of Civil Engineering, Bangladesh University of Engineering and Technology, Dhaka, August
- Islam MM, Choudhury MSI, Abdulla M, Amin AFMS (2011) confinement effect of fiber reinforced polymer wraps in circular and square concrete columns, 4th Annual Paper Meet and 1st Civil Engineering Congress, Civil Engineering Division, Institution of Engineers, Bangladesh (IEB), 22–24 December, Dhaka (Awarded best paper)
- Kachlakev DI, Miller T, Yim S, Chansawat K, Potisuk T (2001) Finite Element Modeling of Reinforced Concrete Structures Strengthened With FRP Laminates, California Polytechnic State University, San Luis Obispo, CA and Oregon State University, Corvallis, OR for Oregon Department of Transportation, May
- Lee S, Cho J, Vecchio FJ (2011) Diverse embedment model for steel fiber-reinforced concrete in tension: model development, *ACI materials Journal*
- Shah SP, Swartz SE, Ouyang C (1995) *Fracture Mechanics of Concrete*. John Wiley & Sons Inc, New York
- Uddin MK, Mustafiz AZ, Chowdhury MA, Mondal P (2013) Investigation of the Flexural Capacity of Beams made of Steel Fiber Reinforced Concrete (SFRC), B.Sc. Engineering Thesis, Department of Civil Engineering, Ahsanullah University of Science and Technology, Dhaka, April
- Willam KJ, Warnke ED (1975) Constitutive Model for the Triaxial Behavior of Concrete. In: *Proceedings, International Association for Bridge and Structural Engineering*, ISMES, Bergamo, Italy, vol 19, pp 1–30

